

## CdTe/MnTe shortperiod superlattices: Elastic properties

E. Abramof, W. Faschinger, H. Sitter, and A. Pesek

Citation: *Appl. Phys. Lett.* **64**, 49 (1994); doi: 10.1063/1.110917

View online: <http://dx.doi.org/10.1063/1.110917>

View Table of Contents: <http://apl.aip.org/resource/1/APPLAB/v64/i1>

Published by the [American Institute of Physics](#).

---

### Additional information on *Appl. Phys. Lett.*

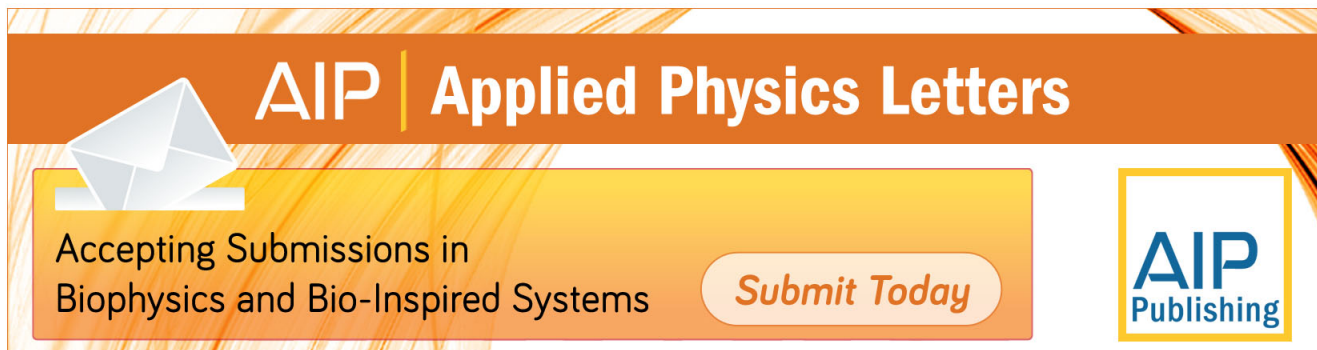
Journal Homepage: <http://apl.aip.org/>

Journal Information: [http://apl.aip.org/about/about\\_the\\_journal](http://apl.aip.org/about/about_the_journal)

Top downloads: [http://apl.aip.org/features/most\\_downloaded](http://apl.aip.org/features/most_downloaded)

Information for Authors: <http://apl.aip.org/authors>

## ADVERTISEMENT



**AIP** | Applied Physics Letters

Accepting Submissions in  
Biophysics and Bio-Inspired Systems

*Submit Today*

**AIP**  
Publishing

# CdTe/MnTe short-period superlattices: Elastic properties

E. Abramof,<sup>a)</sup> W. Faschinger, and H. Sitter  
*Institut für Experimentalphysik, Universität Linz, A-4040 Linz, Austria*

A. Pesek  
*Forschungsinstitut für Optoelectronik, Universität Linz, A-4040 Linz, Austria*

(Received 23 August 1993; accepted for publication 21 October 1993)

We report on the structural characterization of CdTe/MnTe short-period superlattices. The critical thickness of MnTe on CdTe layers was determined by reflection high-energy electron diffraction experiments. Detailed high-resolution x-ray diffraction measurements and the computer simulation of the measured spectra enabled the determination of the zinc blende MnTe elastic properties in the superlattices. The knowledge of these properties allowed the growth of strain balanced CdTe/MnTe superlattices pseudomorphic to a  $\text{Cd}_{0.96}\text{Zn}_{0.04}\text{Te}$  buffer. The superlattices exhibited x-ray linewidths of about 100 arcsec.

Recent interesting neutron diffraction experiments on zinc blende MnTe and II-VI/MnTe superlattices indicated an antiferromagnetic (AFM) type-III structure which strongly depends on the strain state in the magnetic layers. Two examples of these strain effects are: the orientation of the antiferromagnetic sheets is parallel or perpendicular to the layer plane depending if the strain in the magnetic layers of the superlattices is tensile or compressive; the order of the MnTe antiferromagnetic phase transition is changed if the MnTe is a single layer or if it is embedded in the superlattices.<sup>1</sup> These effects together with confinement induced shifts in phonon frequencies studied by Raman scattering<sup>2</sup> have increased the requirement of the determination of the elastic properties of the cubic MnTe in the II-VI/MnTe superlattices in order to clearly establish the strain conditions in these superlattices.

In this work we report on the structural characterization of CdTe/MnTe short-period superlattices. Before growing the superlattices, reflection high-energy electron diffraction (RHEED) experiments were performed to determine the critical thickness of MnTe layers on CdTe. A detailed high-resolution x-ray diffraction (HRXD) investigation on the grown CdTe/MnTe superlattices (SLs) together with the computer simulation of the x-ray spectra using dynamical theory enabled the determination of the elastic properties of the zinc blende MnTe in these SLs. In order to prove that the understanding of the strain conditions can be used to optimize the epitaxial growth, a pseudomorphic strain balanced CdTe/MnTe SL was grown on a  $\text{Cd}_{0.96}\text{Zn}_{0.04}\text{Te}$  buffer with the narrowest x-ray diffraction linewidth reported so far.

The substrates used were semi-insulating [001]-oriented GaAs which have a misorientation of 2° towards the next [110] direction. They were degreased and etched in a solution of  $\text{H}_2\text{SO}_4:\text{H}_2\text{O}_2:\text{H}_2\text{O}=5:1:1$ . The substrates were preheated prior to the growth in order to make the usual oxide desorption. A molecular-beam epitaxy (MBE) system with a background pressure in the growth chamber of  $10^{-9}$  mbar was used. The system is equipped with Zn, Cd, Mn, Te, and Se effusion cells, fast magnetically controlled shutters, a 30

kV RHEED system and a quadrupole mass spectrometer (QMS) with a detection limit up to 511 amu.

Before growing the CdTe/MnTe SLs, RHEED experiments were performed to investigate the growth of MnTe layers. The RHEED patterns of the MnTe surface showed a clear  $(2\times 1)$  reconstruction indicating a Te-stabilized surface. The streaky character of the RHEED pattern, indicating a two-dimensional growth of good quality, is present from the early beginning of the MnTe growth on the CdTe buffer layers. In order to determine the critical thickness of MnTe on CdTe a video camera was installed in front of the RHEED screen to record the RHEED patterns and further analysis with an image processing system was performed. The RHEED patterns of the MnTe surface were recorded with the electron beam along the [110] direction and the RHEED pattern profiles parallel to the shadow edge were evaluated. From the separation between the diffraction streaks in the profiles, the in-plane lattice constant of the MnTe surface was determined. Figure 1 shows the MnTe in-plane lattice constant as a function of the MnTe layer thickness for the growth on CdTe buffer layers. At the beginning of growth, the in-plane lattice constant of MnTe is practically the same as for CdTe and remains constant up to a thickness of ap-

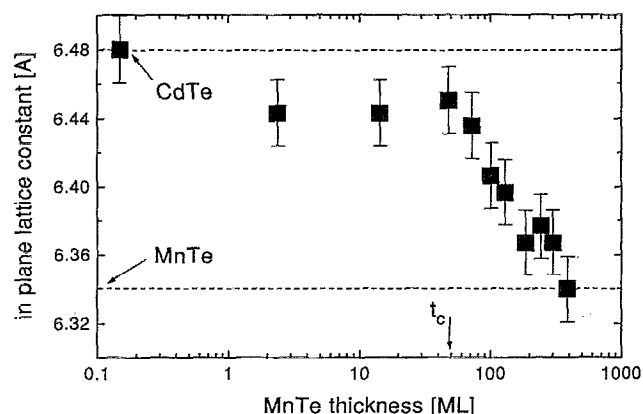


FIG. 1. MnTe in-plane lattice constant as a function of the MnTe layer thickness when growing on CdTe layer. The arrow labeled by  $t_c$  indicates the critical thickness determined by a geometrical model (see Ref. 3).

<sup>a)</sup>Permanent address: Instituto de Pesquisas Espaciais, CP 515, 12201 S. J. dos Campos, SP, Brasil.

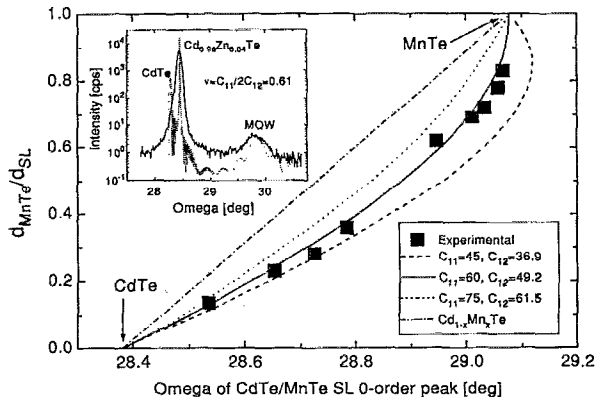


FIG. 2. Composition ( $d_{\text{MnTe}}/d_{\text{SL}}$ ) vs the 0-order satellite peak position of the CdTe/MnTe SLs grown on CdTe buffer layers. The solid, dashed, and dotted curves correspond to the simulated peak position for three different sets of elastic constants  $C_{ij}$  in which the Poisson ratio  $\nu = c_{11}/2c_{12}$  is kept constant at 0.61. The dash-dotted line corresponds to Vergard's law for  $\text{Cd}_{1-x}\text{Mn}_x\text{Te}$  mixed crystals. The insert shows the measured and simulated x-ray spectrum of a MnTe/CdTe multiquantum well grown on  $\text{Cd}_{0.96}\text{Zn}_{0.04}\text{Te}$  buffer from which the Poisson ratio was determined.

proximately 50 ML (160 Å). At this point the layer starts to relax by the formation of misfit dislocations, and at a thickness of about 400 ML the MnTe layer is completely relaxed. A critical thickness of about 50 ML was then determined for the growth of MnTe on CdTe (misfit=0.022). The arrow inserted in the figure indicates the predicted critical thickness obtained from a geometrical model for dislocation generation described in Ref. 3. In this model the critical thickness is given by  $t_c = b/mf$ , where  $b$  is the Burgers vector,  $f$  is the misfit between the layer and the substrate, and  $m$  is a small number between 1 and 2. When taking a Burgers vector of one atomic separation and putting  $m \cong 1$ , the formula simplifies to  $t_c \cong 1/f$  (in units of monolayers). A good agreement between the measured critical thickness of MnTe on CdTe and the one predicted by this model is observed.

To obtain a good control on the growth of the CdTe/MnTe SLs, the CdTe layers were grown by atomic layer epitaxy (ALE) whereas for the MnTe layers we developed a quadrupole mass spectrometer controlled molecular-beam epitaxy which enabled monolayer growth control of the MnTe layers.<sup>4</sup> The CdTe/MnTe SLs samples were grown on a 1- $\mu\text{m}$ -thick (001) CdTe buffer layer, and their average composition was varied between 10% and 80% of Mn content. In all cases the MnTe layer thickness in the SLs was maintained smaller than 40 ML in order to keep it below the critical thickness determined before.

The HRXD system was used to measure the x-ray diffraction spectra of the samples. The period of all grown SLs was calculated from the position of the satellite peaks. An agreement of about 5% between the measured and intended values was obtained. Figure 2 shows the Mn composition in the superlattice, i.e., the ratio between the MnTe layer thickness and the total period of the SL ( $d_{\text{MnTe}}/d_{\text{SL}}$ ), versus the position of the 0-order SL peak for the CdTe/MnTe SLs grown on CdTe buffer layers. The relative tilt between the superlattice and the buffer, which normally appears in the growth on misoriented substrates,<sup>5,6</sup> was also measured and

corrected when plotting the position of the 0-order satellite peak. The dash-dotted straight line between the CdTe and MnTe corresponds to the Vergard's law for the peak position of  $\text{Cd}_{1-x}\text{Mn}_x\text{Te}$  mixed crystals. The deviation of the 0-order satellite peak position from the position of the corresponding mixed crystal is due to strain in the SLs.

In order to get a quantitative understanding of the strain state we simulated the HRXD spectra using dynamical diffraction theory based on the Takagi-Taupin equations.<sup>7</sup> A proper description of a free-standing strained layer SL grown in (001) direction requires the knowledge of the elastic constants  $C_{11}$  and  $C_{12}$  of each SL constituent. These values are known for CdTe, but not for the metastable cubic MnTe. In order to get effective  $C_{ij}$  values for our system we proceeded in the following way: HRXD measurements of a single, fully pseudomorphic film allow a very simple determination of the Poisson ratio  $\nu = C_{11}/2C_{12}$  of a material, however a pseudomorphic MnTe layer on CdTe should not be thicker than about 100 Å, which is too thin to get a pronounced HRXD peak. In order to increase the thickness but retain a pseudomorphic situation we used a strain balanced multi quantum well (4 CdTe wells embedded in 5 MnTe barriers) grown on  $\text{Cd}_{0.96}\text{Zn}_{0.04}\text{Te}$  and a 700-Å-thick CdTe buffer. The compressive strain in the CdTe buffer and quantum wells is intended to partially counterbalance the tensile strain of the MnTe layers. Therefore, it is reasonable to assume that the whole structure is still pseudomorphic, although the overall MnTe thickness is 200 Å, well above the critical thickness of a single MnTe film on CdTe. In such a pseudomorphic structure, the peak position depends only on the assumed Poisson ratio, but not on the individual  $C_{ij}$  values. The measured spectrum of the structure is shown in the insert of Fig. 2, together with the best fit, which was achieved for  $\nu=0.61$ .

Using the Poisson ratio  $\nu$ , we tried to fit the 0-order satellite peak position of the superlattices showed in Fig. 2. The solid, dashed and dotted lines are results of fits where the individual  $C_{ij}$  values were varied, but  $\nu$  was kept constant. A good fit to the data points is achieved for  $C_{11}=60$  and  $C_{12}=49$ . In all calculations the SLs were assumed to be free-standing, i.e., each layer of the SL is completely strained so that the in-plane lattice constant within the SL is the same for CdTe and MnTe, but the SL as a whole is completely relaxed with respect to the buffer. Under this assumption all SLs, which cover nearly the whole range of composition, can be described by the same  $C_{ij}$ . This proves that the strain situation is very similar for all samples, and the determined  $C_{ij}$  are at least good effective values for our sample configuration.

Going one step further, we used this information on critical thicknesses and elastic properties to determine the optimum composition for the growth of a CdTe/MnTe SL which is fully strain balanced with respect to a thick  $\text{Cd}_{0.96}\text{Zn}_{0.04}\text{Te}$  buffer layer grown by hot wall beam epitaxy.<sup>8</sup> Figure 3 shows the HRXD spectrum and the sample configuration. In order to eliminate chemically cleaned interface of the  $\text{Cd}_{0.96}\text{Zn}_{0.04}\text{Te}$  buffer, a pseudomorphic CdTe/ZnTe buffer SL was grown first. This SL has approximately twice the period of the desired CdTe/MnTe SL, so that only every second satellite in the HRXD spectrum originates from the CdTe/

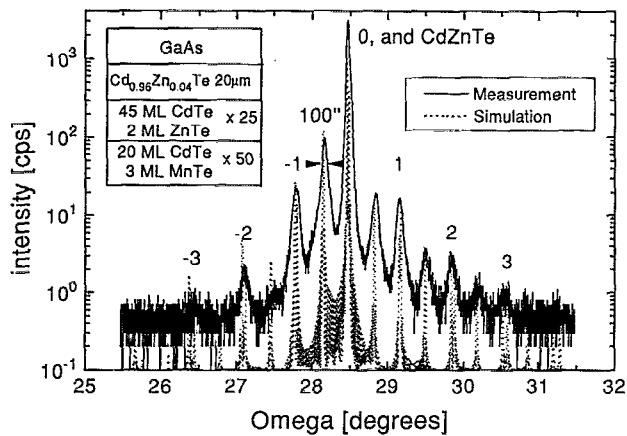


FIG. 3. High-resolution x-ray diffraction spectrum and dynamical simulation of a strain balanced CdTe/MnTe SL grown pseudomorphically on a  $\text{Cd}_{0.96}\text{Zn}_{0.04}\text{Te}$  buffer and a CdTe/ZnTe SL. Details about the structure are shown in the insert. The numbers indicate the order of the satellite peaks of the CdTe/MnTe SL.

MnTe SL (indicated by the numbers in Fig. 3). The SL peaks have a full width at half-maximum of about 100 arcsec, which is the best value reported so far for any SL containing a metastable cubic Mn compound, and no significant broadening of the SL peaks with respect to the CdZnTe buffer peak occurs. This is an indication that the whole structure is in fact pseudomorphic. An x-ray diffraction simulation of the whole structure using the elastic constants determined above is also shown in Fig. 3. The good match between the mea-

sured and simulated x-ray spectrum proves the reliability of the determined  $C_{ij}$  values.

In conclusion, we determined the critical thickness of metastable cubic MnTe by RHEED, and showed that dynamical simulations of high-resolution x-ray diffraction spectra allow a determination of the strain state in CdTe/MnTe superlattices. Elastic constants of metastable cubic MnTe were determined by a best fit procedure. The knowledge of critical thicknesses and elastic properties could be used to grow pseudomorphic strain balanced CdTe/MnTe superlattices with very narrow x-ray diffraction linewidths.

This work was partially supported by the Fonds zur Förderung der wissenschaftlichen Forschung in Österreich (Projects 7261 PHY and 8446 PHY). We thank the Brazilian Research Council CNPq for supporting the Ph.D. scholarship of E. Abramof.

- <sup>1</sup>T. M. Giebultowicz, P. Klosowski, N. Smarth, H. Luo, and J. K. Furdyna, and J. J. Rhyne, *Phys. Rev. B* (in press).
- <sup>2</sup>S. Venugopalan, L. A. Kolodziejcki, R. L. Gunshor, and A. K. Ramdas, *Appl. Phys. Lett.* **45**, 974 (1984).
- <sup>3</sup>D. J. Dunstan, S. Young, and R. H. Dixon, *J. Appl. Phys.* **70**, 3038 (1991).
- <sup>4</sup>E. Abramof, W. Faschinger, H. Sitter, and A. Pesek (to be published).
- <sup>5</sup>A. Pesek, K. Hingerl, F. Riesz, and K. Lischka, *Semicond. Sci. Technol.* **6**, 705 (1991).
- <sup>6</sup>E. Abramof, A. Pesek, P. Juza, H. Sitter, T. Fromherz, and W. Jantsch, *Appl. Phys. Lett.* **60**, 2368 (1992).
- <sup>7</sup>W. J. Bartels, J. Hornstra, and D. L. Lobeek, *Acta Crystallog. Sect. A* **42**, 539 (1986).
- <sup>8</sup>J. Humenberger, H. Sitter, K. Lischka, A. Pesek, and H. Pascher, *The Physics of Semiconductors*, edited by E. M. Anastakis and J. D. Jönsson (World Scientific, Singapore, 1990), p. 312.